KOJAK encodes a cellulose synthase-like protein required for root hair cell morphogenesis in *Arabidopsis*

Bruno Favery,[1,2,4] Eoin Ryan,[1,3,4] Julia Foreman,[1] Paul Linstead,[1] Kurt Boudonck,[1] Martin Steer,[3] Peter Shaw,[1] and Liam Dolan[1,5]

[1]Department of Cell Biology, John Innes Centre, Norwich, NR4 7UH, UK; [2]INRA, Unité Santé Végétale et Environnement, 06600 Antibes, France; [3]Botany Department, University College, Belfield, Dublin 4, Ireland

The cell wall is an important determinant of plant cell form. Here we define a class of *Arabidopsis* root hair mutants with defective cell walls. Plants homozygous for *kojak* (*kjk*) mutations initiate root hairs that rupture at their tip soon after initiation. The *KJK* gene was isolated by positional cloning, and its identity was confirmed by the molecular complementation of the Kjk$^-$ phenotype and the sequence of three *kjk* mutant alleles. *KOJAK* encodes a cellulose synthase-like protein, AtCSLD3. KOJAK/AtCSLD3 is the first member of this subfamily of proteins to be shown to have a function in cell growth. Subcellular localization of the KOJAK/AtCSLD3 protein using a GFP fusion shows that KOJAK/AtCSLD3 is located on the endoplasmic reticulum, indicating that KOJAK/AtCSLD3 is required for the synthesis of a noncellulosic wall polysaccharide. Consistent with the cell specific defect in the roots of *kjk* mutants, *KOJAK/AtCSDL3* is preferentially expressed in hair cells of the epidermis. The Kjk$^-$ phenotype and the pattern of *KOJAK/AtCSLD3* expression suggest that this gene acts early in the process of root hair outgrowth. These results suggest that KOJAK/AtCSLD3 is involved in the biosynthesis of β-glucan-containing polysaccharides that are required during root hair elongation.

[*Key Words*: *Arabidopsis*; cell wall; cellulose synthase-like gene; β-glucan; root hair; morphogenesis]

Received September 4, 2000; revised version accepted November 2, 2000.

Cell morphogenesis is the process by which postmitotic cells attain their final form and is responsible for the diversity of cell morphologies found in plants. Spatially controlled and cell-specific cell wall deposition is a major determinant of plant cell form. Few genes involved in determining plant cell shape have been characterized at the molecular level. It is clear the cytoskeleton is a major determinant of cell shape (Mathur and Chua 2000), and genetic analysis of the *ZWICHEL* (*ZWI*) gene has defined a role for a class of kinesin-related proteins in the formation of the stellate trichome of the shoot epidermis of *Arabidopsis* (Oppenheimer et al. 1997). The swollen cell phenotype of plants homozygous for loss of function mutations in the *RADIAL SWELLING1* (*RSW1*) gene illustrates the role of cell wall cellulose in the establishment and maintenance of cell shape (Arioli et al. 1998). Cellulose, which is a major component of the cell wall, is synthesized at the plasma membrane. Matrix polysaccharides that constitute the noncellulosic wall fraction, such as xyloglucan and pectin, are synthesized in the endomembrane system of the cell and are delivered to the cell surface in Golgi-derived vesicles. Little is known about the enzymes responsible for the biosynthesis of wall polysaccharide components. None of the enzymes associated with the synthesis of xyloglucan backbone, xylan, or callose has yet been isolated. To understand the molecular mechanism underpinning wall formation during cell growth in plants, we have identified a set of root hair mutants in *Arabidopsis thaliana* with defective cell walls.

The *Arabidopsis* root hair has been used to genetically dissect the process of cellular morphogenesis in plants. Root hairs are tubular extensions that form on the outer surface of specialized epidermal cells called trichoblasts (Schiefelbein and Somerville 1990; Dolan et al. 1994). Hairs play important roles in a diverse array of processes including water and ion uptake and anchorage and are the site of interaction with a range of symbiotic microorganisms. The first stage of root hair morphogenesis involves a change in the polarity of cell growth leading to the formation of a bulge at the distal end of the trichoblast. Bulge formation is accompanied by local cell wall

[4]These authors contributed equally to this work.
[5]Corresponding author.
E-MAIL liam.dolan@bbsrc.ac.uk; FAX 44-1603-450022.
Article and publication are at www.genesdev.org/cgi/doi/10.1101/gad.188801.

thinning and a decrease in apoplastic pH that may be required for the modification of cell wall polymers (Bibikova et al. 1998). A polarized cytoplasm organizes in this protrusion with the formation of a characteristic tip growth morphology when the hair is 20–40 μm in length. The tip is a site of localized cell wall synthesis through an accumulation of secretory vesicles containing protein and polysaccharide polymers. Once tip growth is established, the hair continues to grow, generating a long tubular-shaped cell. Physiological studies have shown that a tip-focused calcium influx generates a cytosolic Ca^{2+} gradient necessary for root hair growth (Schiefelbein et al. 1992; Wymer et al. 1997). Growth ceases on vacuolation of the hair tip.

The genetic analysis of root hair development has identified several genes that are required for the initiation and growth of the root hair. *RHL1*, *RHL2*, and *RHL3* genes are active during the formation of a bulge early in root hair growth. *RHL1* encodes a nuclear protein of unknown function that is required for the formation of the polarized outgrowth (Schneider et al. 1998). *RHD6* activity is necessary to localize the site of hair initiation in the trichoblast. *RHD6* acts through an auxin/ethylene pathway, as the *rhd6* mutant phenotype can be rescued by the application of either auxin or ethylene (Masucci and Schiefelbein 1994). RHD1 strengthens the cell wall in the vicinity of the bulge (Schiefelbein and Somerville 1990). *RHD2* is necessary for hair outgrowth, as plants homozygous for recessive loss of function alleles stop growing soon after the formation of a bulge (Schiefelbein and Somerville 1990). Later-acting genes such as *COW1* (Grierson et al. 1997), *TIP1* (Ryan et al. 1998), and *RHD3* (Galway et al. 1997), and *RHD4* are active in the maintenance of hair elongation and polarity (Schiefelbein and Somerville 1990). *RHD3* encodes a protein with GTP-binding motifs that may be involved in cell signaling during hair formation, its precise role has not been characterized (Wang et al. 1997). While genetic analysis has defined a set of genes required for root hair morphogenesis, the molecular basis of hair outgrowth is still far from being understood.

To identify genes required for cell wall biosynthesis during cell growth, we screened our root hair mutant collection for phenotypes that resemble root hairs treated with an inhibitor of cellulose synthesis, 2,6-dichlorobenzonitrile (DCB; Delmer et al. 1987). DCB-treated root hairs rupture at their tip because of the uncoupling of cellulose biosynthesis and protoplast growth (L. Dolan, unpubl). Here we report the identification of an *A. thaliana* cellulose synthase-like protein, AtCSLD3, encoded by the *KOJAK* gene that is required for the formation of the cell wall during root hair morphogenesis.

Results

Root hairs of kjk *mutants rupture soon after initiation*

Arabidopsis root hairs grown in the presence of the cellulose synthesis inhibitor DCB (2,6-dichlorobenzonitrile) rupture at their tips (data not shown). To identify mutants with cell wall defects, we screened our collection of *Arabidopsis* root hair mutants for ruptured root hair phenotypes. In this screen, one line (D4225) was isolated from a *Ds* transposon-mutagenized Landsberg *erecta* (L*er*) population (Bancroft et al. 1992), and two lines, E1025 and E1100, were isolated from an EMS-mutagenized Columbia (Col) population. The progeny of pairwise combinations of crosses between these mutants had mutant phenotypes indicating that the mutations in these lines are alleles of a single gene. This gene was named *KOJAK* (*KJK*) because of the bald phenotype of the mutant roots. Lines D4225, E1025, and E1100 were designated *kjk-1*, *kjk-2*, and *kjk-3*, respectively. Backcrosses of each of the *kjk* mutants to their respective wild type produced F_1 plants with wild-type phenotypes. The 3:1 segregation of Kjk^+ and Kjk^- plants in the F_2 generation of these backcrosses indicated that the mutations segregate as single recessive alleles. Linkage analysis showed that the *kjk-1* mutation was not caused by the insertion of a *Ds* transposon. All F_1 plants derived from the cross between plants homozygous for *kjk* and plants homozygous for previously published mutations in root hair growth (*rhd1*, *rhd2*, *rhd3*, *rhd4*, *rhd6*, *tip1*, and *cow1*) had wild-type root hair phenotypes indicating that *kjk* defines a new gene required for root hair growth.

Plants homozygous for any *kjk* allele formed no hairs (Fig. 1), although deformed root hairs were occasionally observed. During normal root hair development, the trichoblast produced a small swelling (bulge) at the end of the cell nearest the meristem, from which a tip growing hair emerged. *kjk* mutants produced the initial bulge but failed to develop a root hair. Instead, the bulge continued to swell spherically until it burst eventually, re-

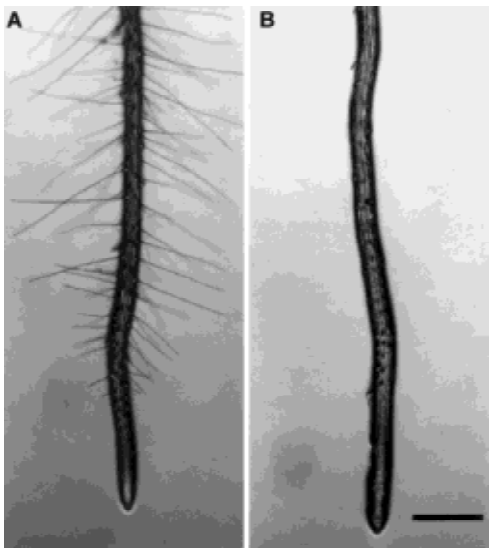

Figure 1. Plants homozygous for the *kjk* mutation do not form root hairs. (*A*) Elongated root hairs are visible on the wild-type (L*er* ecotype) root. (*B*) Plants homozygous for the *kjk-1* mutation do not form root hairs. The characteristic bulges are visible in the early differentiation zone. Scale bar, 100 μm.

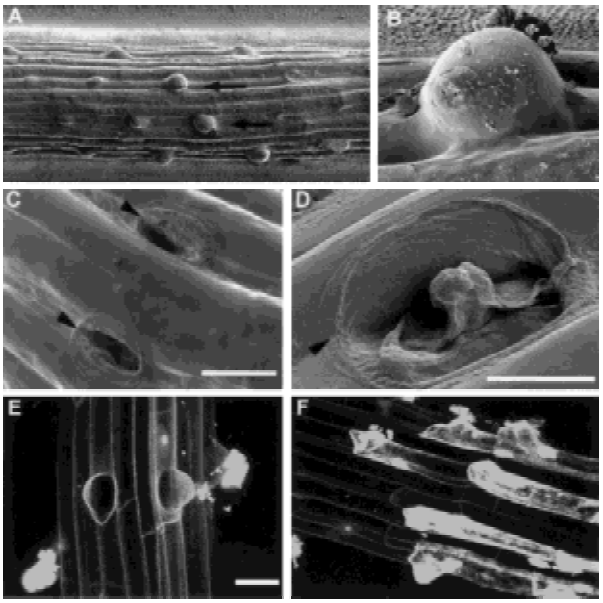

Figure 2. Root hairs swell and burst soon after initiation in plants homozygous for the *kjk* mutation. (*A–D*) Cryo-Scanning electron micrographs of roots of plants homozygous for the *kjk-1* mutation show that the outer wall of the trichoblast swells (arrows) excessively (*A*). The bulge continues to swell until it bursts (*B*), killing the trichoblasts (arrowheads) (*C*,*D*). (*E*,*F*) Confocal images of the root homozygous for the *kjk* mutation stained with propidium iodide, which stains the intercellular spaces between living cells and the contents of dead cells (*E*). Stripes of compressed dead trichoblasts between nonhair epidermal cell files (*F*). Scale bars, 10 mm.

sulting in the extrusion of the protoplast through a fracture in the wall (Fig. 2A–D). The rupture always formed near the dome of the bulge. The dead cells were visualized because of the staining of their cytoplasmic constituents with propidium iodide, which is normally restricted to the cell wall of living cells (Fig. 2E,F). Files of stained cells indicated that every hair cell in the file undergoes lysis (Fig. 2F). These files were located over the anticlinal cell walls of underlying cortical cells (the location in which hair cells normally develop), indicating that *KJK* played no role in the specification of root epidermal cell identity. The gross morphology of the shoot system of *kjk* mutants was indistinguishable from wild type.

kjk *is epistatic to cow1*

To characterize the role of *KJK* in root hair morphogenesis, double mutants comprising *kjk* and other mutants with defects in root hair elongation were constructed. Double mutants were identified in the F_2 populations of crosses between *kjk* and the respective root hair mutant and verified by backcrossing to both parents (test cross; Fig. 3). *kjk* and *rhd2* single mutants had identical phenotypes. The phenotype of the *kjk rhd2* double mutant was indistinguishable from either parent, indicating that two genes may act at the same stage of development. *rhd6* mutants develop few hairs that originate in variable positions along the trichoblast. In roots of seedlings homozygous for both *kjk* and *rhd6*, small bulges were produced in place of hairs as in the *kjk* mutant, but they form in variable positions along the trichoblast as in the *rhd6* single mutant. This additive phenotype indicates that *KJK* activity is required for the growth of root hairs in the *rhd6* background (Fig. 3B–F). While the *rhd1* mutant produced root hairs with excessive bulges at the base (Fig. 3C; Schiefelbein and Somerville 1990), the entire outer cell wall of the *kjk rhd1* trichoblast was swollen, and no root hairs were formed (Fig. 3G). *tip1* root hairs were shorter and more branched than wild type, whereas *kjk tip1* double mutants developed short, thickened root hairs (Fig. 3D–H). Hairs on *rhd3* mutants were wavy, and hairs on *rhd4* plants formed bulges and constrictions along their length. *kjk rhd3* double mutants had very short, slightly wavy root hairs, and *kjk rhd4* had shortened root hairs with bulges and constrictions along their length (data not shown). The double mutants with *rhd1*, *tip1*, *rhd3*, and *rhd4* had intermediate phenotypes with characteristics of each single mutant, indicating that *KJK* acts independent of these genes. Interestingly, the cell-rupture phenotype of *kjk* mutants is suppressed by *tip1*, *rhd1*, *rhd3*, and *rhd4*. *cow1* root hairs were shorter and branch more often than wild type. *kjk* is epistatic to *cow1*; that is, double mutant displayed a Kjk$^-$ phenotype, indicating that these genes act in the same pathway, perhaps with *KJK* acting earlier in hair growth.

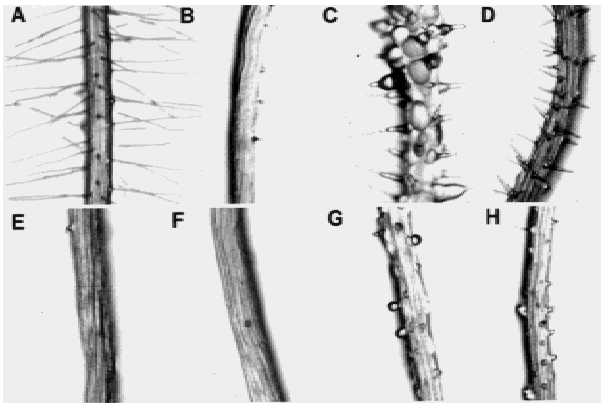

Figure 3. Root phenotype of double mutants. (*A*) Root hairs of the wild-type root. (*B–E*) Single mutant phenotypes and (*F–H*) double mutant phenotypes. Roots of plants homozygous for *rhd6-1* (*B*) are largely hairless. Plants homozygous for the *rhd1-1* mutation (*C*) produce hairs with excessive swellings at its base. Trichoblasts of plants homozygous for *tip1* (*D*) can produce up to three short, branched root hairs. Characteristic bulges on the root of a plant homozygous for the *kjk-2* mutation (*E*). Those hairs that form on roots of plants homozygous for both *kjk-2* and *rhd6* are short (*F*). The entire outer cell wall of the trichoblast of a plant homozygous for both *kjk-2* and *rhd11* is swollen (*G*), but trichoblasts neither rupture nor form a hair. Roots of plants homozygous for both *kjk-1* and *tip1-2* (*H*) produce a few abnormal root hairs.

Molecular cloning of the KJK *gene*

The *KJK* gene was cloned using a map-based cloning strategy. A segregating F_2 family was made from a cross between plants homozygous for the *kjk-1* mutation in the L*er* background and wild-type Col plants. *kjk-1* was initially mapped to the top of chromosome 3 between SSLP markers nga32 and nga172 (Bell and Ecker 1994) using a population of 80 chromosomes (Fig. 4A). Analysis of a further 200 chromosomes identified a single recombination event between nga172 and *kjk-1* whereas no recombinants were identified between *kjk-1* and CAPS marker 17D8LE (Bartel and Fink 1995). Examination of BAC sequences in this region identified a gene encoding a cellulose synthase-like (CSL) protein, *AtCSLD3*. Using a CAPS marker in the *AtCSLD3* gene (CSL, see Material and Methods) that identified a polymorphism between L*er* and Col, we found no recombinants between CSL and *kjk-1* in the population of 220 chromosomes.

To show that *AtCSLD3* encodes the gene that is defective in the *kjk-1* mutant, we transformed plants homozygous for the *kjk-1* mutation with a 7.2-kb *Avr*II genomic fragment that includes the entire *AtCSLD3* gene (Fig. 4B). Twelve independent primary transformants selected on kanamycin had a wild-type root hair phenotype (data not shown). Examination of T_2 plants showed the cosegregation of the kanamycin resistance with the wild-type phenotype. This result provides firm genetic evidence that the Kjk$^-$ phenotype is caused by mutation in the *AtCSLD3* gene. This gene is hereafter designated *KOJAK/Arabidopsis thaliana cellulose synthase-like protein D3* (*KJK/AtCSLD3*). Using the first exon of *KJK/AtCSLD3* as a probe on a Southern blot of L*er* genomic DNA, we showed that there is a single copy of the gene per haploid genome (data not shown).

The *KJK/AtCSLD3* cDNA was cloned by RACE PCR (Frohman et al. 1988). One transcript was detected. The *KJK/AtCSLD3* cDNA is 3819 nucleotides long with an open reading frame (ORF) of 1145 amino acids (Fig. 4B). Translation was assumed to begin at nucleotide 249, the first ATG codon of the open reading frame. Blast searching (Altschul et al. 1997) the Stanford *A. thaliana* database identified similar (99% identical at nucleotide level) expressed sequence tags from *A. thaliana* (Fig. 4B). Comparison of cDNA and genomic sequences revealed that the *KJK/AtCSLD3* gene has three introns, including one in the 5′UTR (Fig. 4B).

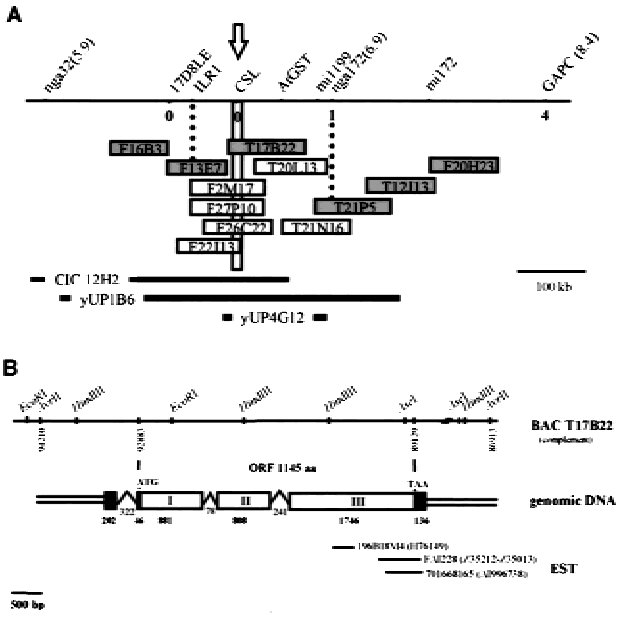

Figure 4. Mapping of the *kjk* mutation and organization of the *KJK/AtCSLD3* gene. (*A*) *KJK* is located on the top of chromosome 3. Adjacent SSLP and CAPS markers with genetic distances are indicated. The number of recombinants identified from a population of 200 mutant chromosomes is given above the respective loci. The vertical bar indicates the region of chromosome 3 containing the *AtCSLD3* gene. The positions of BAC and YAC clones spanning this region are indicated. The sequenced BACs are represented by filled rectangles. (*B*) The restriction map of the *KJK/AtCSLD3* gene is aligned with a graphical representation of the structure of the *KJK/AtCSLD3* gene. Open boxes are exons (I to III, determinated from cDNA) and the gap between is introns. Shaded boxes indicate untranslated sequences. ATG (start codon), TGA (stop codon) and *Arabidopsis* ESTs showing identities with the gene are indicated.

KJK *encodes a cellulose synthase-like protein*

Analysis of the deduced amino acid sequence of *KJK/AtCSLD3* showed that it is a member of the D subfamily of cellulose synthase-like (CSL) genes identified in *A. thaliana* (Cutler and Somerville 1997). The KJK/AtCSLD3 amino acid sequence shares 64%–68% identity and 76%–81% similarity with the other four CSLD members (CSLD1, D2, D4, and D5; Fig. 5A). The KJK/AtCSLD3 protein is similar in size to several cellulose synthase catalytic subunit proteins (CESA). These include the *Arabidopsis* RSW1, ATHA, ATHB (Arioli et al. 1998), IRX3 (Taylor et al. 1999), and ARAXCELA (Wu et al. 1998); the cotton CELA1 (GhCESA1; Pear et al. 1996); and PtCESA2 from *Populus tremuloides*. The CSLD family constitutes a distinct lineage among the CESA and AtCSL proteins (Fig. 5B).

Alignment of sequences shows that several regions in the KJK/AtCSLD3 protein are conserved in the plant CESA and *Arabidopsis* CSLD proteins (Fig. 5A–C). KJK/AtCSLD3 contains the four highly conserved subdomains (U-1 through U-4) that characterize the processive β-glycosyl transferases in plants and bacteria (Saxena et al. 1995; Pear et al. 1996). These regions contain the three conserved aspartate (D) residues and the QxxRW motif that have been proposed to be involved in substrate (UDP-glucose) binding and/or catalysis (Fig. 5A–C). Surrounding these motifs, KJK/AtCSLD3 shares one plant-specific, conserved region (P-CR) and one hypervariable region (HVR) with plant CESA proteins (Fig. 5C; Pear et al. 1996; Arioli et al. 1998; Delmer 1999; Taylor et al. 1999). However, KJK/AtCSLD3 has additional amino acids in the P-CR domain (Fig. 5A). These additional amino acids are only found in the AtCSLD protein

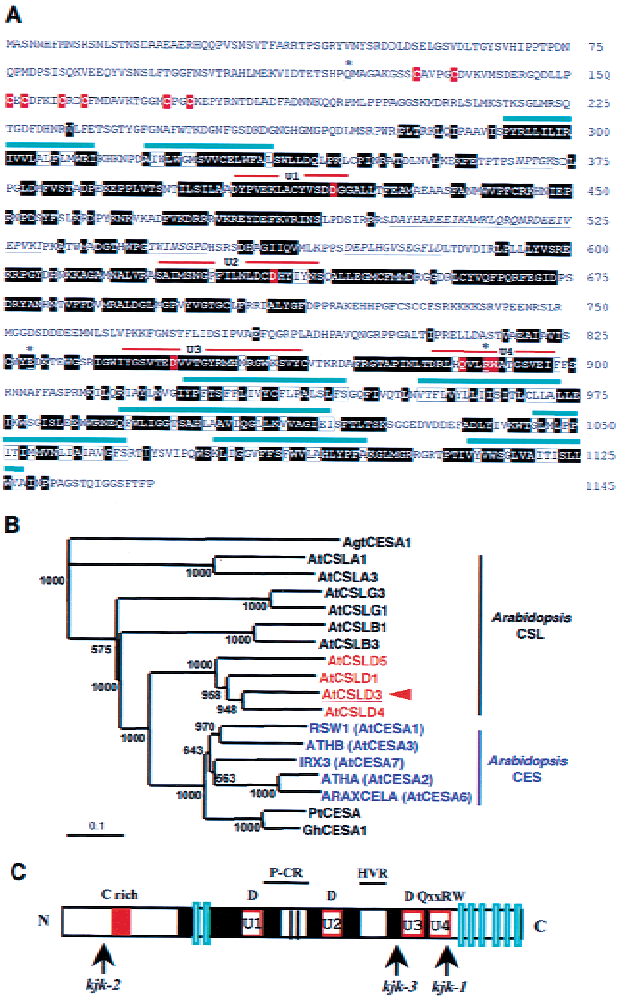

Figure 5. *KJK* encodes a cellulose synthase-like protein. (*A*) Amino acids sequence of the KJK/AtCSLD3 protein. Conserved residues (white letters) between *Arabidopsis* cellulose synthase-like AtCSLD (AtCSLD1, AtCSLD4, AtCSLD5) and CESA members from *Arabidopsis thaliana* (ATHA, ATHB, RSW1, IRX3, ARAXCELA), *Populus tremuloides* (PtCESA2) and *Gossypium hirsutum* (GhCESA1). Additional amino acids present in AtCSLD subfamily are underlined and italicized. The position of the cysteine-rich region (C in red), the eight presumed transmembrane segments (green upperlining), the conserved subdomains U1 to U4 (red upperlining) that contain the three D residues and the QxxRW (in red) signature are indicated. The position of the three *kjk* mutations (amino acids Q^{121}, R^{889}, substituted by stop codon in *kjk-2* and *kjk-1* alleles, respectively, and E^{830}–K substitution in *kjk-3*) are indicated by an asterisk. (*B*) Schematic representation of KJK/AtCSLD3 structure. Shaded boxes represent conserved sequences. The cysteine-rich region, the U1 to U2 subdomains, the plant-specific and conserved region (P-CR), and the plant hypervariable region (HVR) are indicated. (*C*) Relationship tree of CESA and AtCSL subfamilies (A, B, D, and G) products. *Agrobacterium tumefaciens* CELA (AgtCESA1) was used to root the tree.

subfamily. The region close to the N terminus contains a cysteine-rich region (Fig. 5A–C), which has been suggested to form a zinc finger–binding domain involved in protein–protein interactions (Delmer 1999). This motif is also present in CESA cellulose synthases (Pear et al. 1996; Arioli et al. 1998; Taylor et al. 1999) but is located closer to the N-terminal region. Therefore, KJK/AtCSLD3 is likely to be involved in the synthesis of cellulose or other related β-glycans (Cutler and Somerville 1997).

Molecular analysis of the kjk *mutant alleles*

To define the molecular basis for the *kjk* mutations, the genomic DNA sequence of the three *kjk* mutant alleles was determined. We identified a single mutation in each of the mutant alleles. *kjk-1* has a C to T transition, which results in the introduction of a stop codon in place of the arginine (R) at position 889 in the conserved QxxRW motif (Fig. 5A–C). *kjk-2* has a stop codon in place of the glutamine (Q) at position 121, which is predicted to cause premature termination of translation. *kjk-2* is a putative complete loss of function mutation. *kjk-3* has a G to A transition, resulting in a change of a glutamic acid (E) to a lysine (K) at position 830 close to the conserved U3 segment (Fig. 5A–C).

KJK encodes a membrane protein located in the endoplasmic reticulum

Analysis of peptide structure and hydrophobicity predicted that KJK/AtCSLD3 has eight membrane-spanning domains. Two transmembrane segments are located between residues 292–312 and 319–335, and six further transmembrane segments are detected in the C-terminal region between residues 926 and 1129 (Fig. 5A–C). KJK/AtCSLD3 has no obvious N-terminal signal sequence. These data suggest that KJK/AtCSLD3 is a membrane protein anchored to the plasma membrane, as predicted for a cellulose synthase catalytic subunit, or to a membrane in the endomembrane system. Subcellular localization of KJK/AtCSLD3 protein was determined in vivo using a translational fusion between *KJK/AtCSLD3* and the green fluorescent protein 4 (GFP4). The *KJK/AtCSLD3*::*mGFP4* construct under the control of the constitutive 35S promoter was delivered into *Nicotiana benthamiana* leaf cells by a transient *Agrobacterium* infiltration assay. All infiltrated epidermal cells showed that the KJK/AtCSLD3–GFP4 fusion protein was present in the endoplasmic reticulum that is located in the thin layer of cytoplasm between the plasma membrane and the vacuole (Fig. 6A–D). No KJK/AtCSLD3–GFP4 was detected in the plasma membrane, but it is possible that small amounts were present that we were unable to detect. The KJK/AtCSLD3–GFP4 fusion protein was excluded from vacuoles, organelles, and nucleus, and no free cytoplasmic fluorescence was detected. A similar subcellular distribution was observed in cells that were transformed with a GFP4 that is targeted specifically to the endoplasmic reticulum (ER-GFP4; Fig. 6E), as described previously (Haseloff et al. 1995). Cells transformed with GFP4 alone, which is located in the cyto-

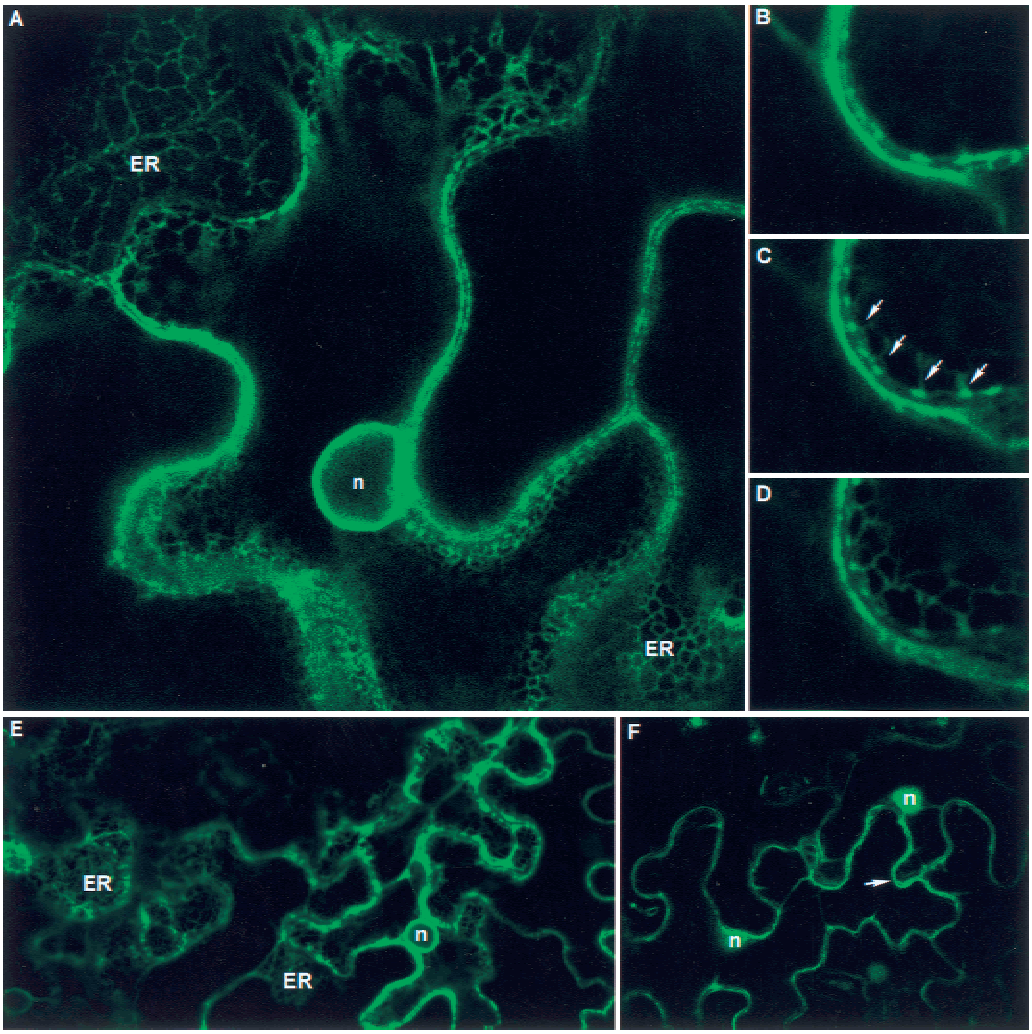

Figure 6. Subcellular localization of the KJK/AtCSLD3 protein using GFP. Tobacco epidermis was infiltrated with *Agrobacterium tumefaciens* containing a binary vector with the 35S promoter and GFP fusion. (*A–D*) Confocal sections of transformed epidermal cells. KJK/AtCSLD3-GFP fusion protein is located in the endoplasmic reticulum (ER) (*A*). Successive 1-μm confocal sections (*B*,*C*,*D*) show that GFP fluorescence is located in the endoplasmic reticulum (arrows). A similar subcellular distribution was observed with the control ER-targeted GFP (*E*). The cytoplasmic GFP is distributed throughout the cytoplasm (arrow) restricted between the vacuole and the cell wall (*F*). (ER) Endoplasmic reticulum; (n) nucleus.

plasm and the nucleus, are shown for comparison (Fig. 6F). These data suggest that KJK/AtCSLD3 is located in the ER membrane.

Expression pattern of KJK

Steady-state levels of *KJK/AtCSLD3* mRNA were examined by Northern blot and RT–PCR analysis. Northern blot analysis failed to detect *KJK/AtCSLD3* transcripts. In contrast, RT–PCR showed that this gene is expressed throughout the wild-type plant. Signal was detected in leaves, roots, stems, and inflorescences (Fig. 7A). *KJK/AtCSLD3* gene expression was also characterized in mutants homozygous for the three alleles to examine the effect of these mutations on *KJK/AtCSLD3* mRNA accumulation. A dramatic reduction in the abundance of the transcript was detected in seedlings homozygous for the *kjk-2* allele (data not shown). Wild-type levels of *KJK/AtCSLD3* mRNA were observed in seedlings homozygous for *kjk-1* and *kjk-3*, which implies that these mutations alter KJK/AtCSLD3 protein function but not *KJK/AtCSLD3* transcript synthesis or stability.

To determine the cells in which *KJK/AtCSLD3* is expressed, the *KJK/AtCSLD3* gene and its native promoter were fused to the endoplasmic reticulum targeted-GFP2.5 (ERGFP2.5). Images of roots from transformed wild-type plants showed that *KJK/AtCSLD3–ERGFP2.5* fusion is preferentially expressed in the root hair cells (Fig. 7B,C). *KJK/AtCSLD3* expression is first detected in cells at the early stages of root hair growth—during the formation of the bulge—and continues to be expressed in growing root hairs. *KJK/AtCSLD3* is occasionally expressed at much lower levels in non–root hair epidermal cells (Fig. 7C) and in lateral root cap cells (data not

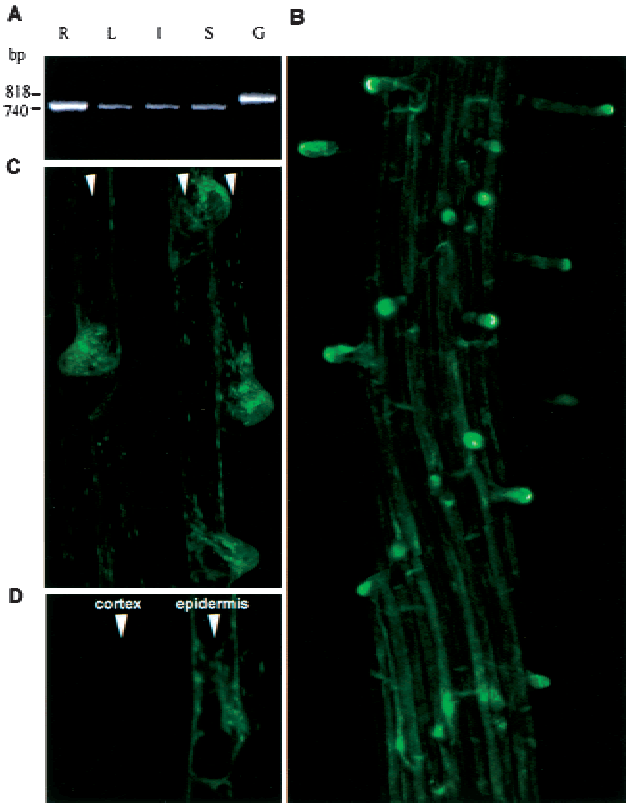

Figure 7. Analysis of *KJK/AtCSLD3* expression. (*A*) RT–PCR analysis of *KJK/AtCSLD3*. Total RNA was isolated from roots (R), leaves (L), inflorescences (I), and inflorescence stems (S) of wild-type plants. Wild-type genomic DNA (G) was used as control. (*B–D*) Projections of confocal images of a 5-d-old wild-type seedling transformed with *KJK/AtCSLD3::GFP*. GFP fluorescence is detected preferentially in root hair cells (arrowheads) (*B*). Weak *KJK/AtCSLD3* expression is visualized in the nonhair epidermal cells (*C*). No expression was detected in cortical cells (*D*).

shown). No expression was observed in the cortical or endodermal cells (Fig. 7D) or vascular cylinder (data not shown). No GFP fluorescence was detected in the shoot meristem, cotyledons, or leaves of young seedlings, indicating that *KJK/AtCSLD3* is not expressed at this stage of shoot development (infloresencences were not examined in this study). Thus, *KJK/AtCSLD3* is preferentially expressed in growing root hair cells in the root, consistent with its requirement in root hair cell expansion. The *KJK/AtCSLD3–ERGFP2.5* construct did not complement the Kjk$^-$ phenotype when transformed into plants homozygous for the *kjk* mutation. This is not unexpected, as the GFP2.5 is itself targeted to the ER and may therefore have altered the topology or function of the KJK/AtCSLD3 protein.

Discussion

A screen for cell wall mutants in *A. thaliana* using a root hair rupture phenotype led to the isolation of three recessive alleles in the *KJK* gene. *KJK* was cloned and found to encode a cellulose synthase-like protein, KJK/AtCSLD3, required for the formation of an intact cell wall during root hair morphogenesis. This is the first report of the isolation and characterization of a cellulose synthase-like protein involved in wall formation during root hair morphogenesis. *KJK/AtCSLD3* is one of a battery of effector genes that are likely to be targets of the transcription factor cascade that has been shown to be involved in the specification of cell identity in the root epidermis (Lee and Schiefelbein 1999). Other targets of these transcriptional regulators will be involved in the cellular functions required for the growth and shaping of the root hair cell.

KJK *gene is required for root hair cell morphogenesis*

One of the earliest stages of root hair growth is the formation of a bulge on the outer face of the trichoblast from which a tip growing root hair emerges. In plants homozygous for each of the three *kjk* mutations, root hairs initiate in the correct position on the trichoblast but tip growth is not established. Instead, the bulge continues to expand slowly and eventually ruptures. DCB, a cellulose synthase inhibitor, which also causes hair cell rupture, phenocopies this mutation. This suggests that hairs of plants homozygous for *kjk* mutations have a localized cell wall defect resulting in the formation of a weakened wall. *KJK/AtCSLD3* is required at or before the establishment of tip growth for the maintenance of the integrity of the cell wall, and in the absence of *KJK/AtCSLD3* activity, the cell wall cannot withstand the internal pressure of the growing protoplast.

KJK *acts early in the temporal sequence of hair growth*

A number of other genes required for root hair morphogenesis have been described in *Arabidopsis*. Only *RHL1* and *RHD3* have been cloned. *RHL1* encodes a nuclear protein of unknown function (Schneider et al. 1998), and *RHD3* encodes a G-protein of unknown function (Wang et al. 1997). The Kjk$^-$ phenotype indicates that KJK/AtCSLD3 acts early in the temporal sequence of hair growth. *kjk* is epistatic to *cow1*, suggesting that these genes act in the same pathway. Alternatively, *KJK/AtCSLD3* activity may be needed before *COW1* activity is required during hair growth. *KJK/AtCSLD3* and *RHD2* genes are both required at the same stage of development for the transition from swelling formation to tip-growth. *RHD2* is required for the formation of the Ca^{2+} gradient, although it is as yet unclear what *RHD2* encodes (Bibikova et al. 1998). The intermediate phenotype of the double mutants with root hair morphogenesis mutants *rhd1*, *rhd3*, *rhd4*, and *tip1* suggests that *KJK/AtCSLD3* acts independently of these genes. It is probable that these genes act independently at the same stage of hair elongation. Interestingly, these mutations suppress cell rupture of root hairs in double mutants. The slow growth rate of these mutant root hairs may decrease the expan-

sive pressure on the cell wall of *kjk* hairs and thereby suppress the rupturing. It is nevertheless formally possible that the respective gene products interact directly in the developing root hair cell.

KJK *is a member of the cellulose synthase-like family*

The sequence of *KJK/AtCSLD3* indicates that it encodes a protein similar to processive β-glycosyltransferases that catalyze the transfer of multiple sugar residues from an activated donor substrate to an acceptor molecule. *KJK/AtCSLD3* is a member of a multigene family in *Arabidopsis* that is similar to the catalytic subunit responsible for the synthesis of cellulose (CESA; Cutler and Somerville 1997). More than 40 members have been identified in the *Arabidopsis* genome. These cellulose synthase-like (CSL) genes were classified into five subfamilies: *AtCSLA*, *AtCSLB*, *AtCSLD*, *AtCSLE*, and *AtCSLG*. The hydrophobicity plots of CESA and CSL members predict a structure that is generally similar for each with a number of membrane-spanning domains and highly conserved subdomains U-1 through U-4, which are proposed to be involved in substrate (UDP-glucose) binding and/or catalysis.

We identified mutations in the *KJK/AtCSLD3* sequence in each of the different alleles. Plants homozygous for each of the *kjk* alleles have indistinguishable root hair phenotypes. *kjk-1* and *kjk-2* are predicted to encode truncated proteins. *kjk-2* has a stop codon near the N terminus and low levels of expression indicating that it is a complete loss of function allele. The U-4 conserved subdomain and the six C terminus transmembrane domains that are missing in *kjk-1* are therefore essential for function. The missense mutation representing change in one amino acid was found in *kjk-3*, demonstrating a functional role for this residue (E^{830}).

Plant CESA homologs were first identified from developing cotton fibers (Pear et al. 1996). However, the proof of function in vivo of plant CESA genes was established recently by the characterization of two *Arabidopsis* mutants defective in cellulose deposition. The temperature-sensitive mutant *radial swelling1* (*rsw1*) has a reduction in cellulose content, an accumulation of noncrystalline β-1,4-glucan, and morphological abnormalities (Arioli et al. 1998). The *irregular xylem3* (*irx3*) mutant has collapsed xylem vessels and decreased cellulose content in inflorescence stems (Turner and Somerville 1997; Taylor et al. 1999).

KJK/AtCSLD3 *is located in the endoplasmic reticulum*

The primary structure of *KJK/AtCSLD3* predicts that it is a membrane protein located in the endomembrane system or plasma membrane. Expression of KJK/AtCSLD3 fused to GFP indicated that KJK/AtCSLD3 is located in the endoplasmic reticulum. The endoplasmic reticulum plays a central role in the biosynthesis of the macromolecules. Many lipids, glycoproteins, and polysaccharides originate in the endoplasmic reticulum and are progressively modified as they move via the Golgi to the plasma membrane. However, we cannot entirely rule out the possibility that low levels of KJK/AtCSLD3 are also present in the plasma membrane or in the Golgi apparatus, which is known to contain glycosyltransferase activities. We are currently generating antibodies to the KJK/AtCSLD3 protein to further characterize it's subcellular distribution.

Role of KJK/AtCSLD3 *in wall biosynthesis of the root hair cell*

KJK/AtCSLD3 mRNA preferentially accumulates in growing root hair cells and consequently may be involved in cell type–specific β-glucan synthesis. This early and localized expression in the root hair cell is consistent with the mutant phenotype and with the proposed role for KJK/AtCSLD3 in the establishment of the growth of the hair. The plant primary cell wall is composed of a network cellulose microfibrils embedded in a Golgi-derived matrix of hemicellulose, pectins, and proteins. Hemicellulose, pectin, and proteins are processed in the endomembrane system secreted into incipient cell plate and subsequently into the cell wall proper. In contrast, cellulose microfibrils are synthesized in terminal complexes at the plasma membrane (Brown et al. 1996; Kimura et al. 1999).

Whereas KJK/AtCSLD3 is similar to CESA and therefore may be involved in cellulose biosynthesis, its subcellular localization in the endoplasmic reticulum suggests that AtCSLD3 functions in the biosynthesis of other polysaccharides. These include β-xylans, mannans, or the backbone of xyloglucan (Cutler and Somerville 1997; Carpita and Vergara 1998; Delmer 1999). The biochemical analysis of the cell wall of *kjk* roots will allow the elucidation of the precise function of *KJK/AtCSLD3* in the biosynthesis of the cell wall. It is to be anticipated that a defect in *KJK/AtCSLD3* will result in a wall with an altered composition, structure, and rheological properties. Unfortunately, the cell-specific phenotype of plants homozygous for *kjk* mutations makes the analysis of the biochemical defect in the wall of mutants difficult. Future experiments in which *KJK/AtCSLD3* is mis- or overexpressed may obviate this problem and identify the precise biochemical function of KJK/AtCSLD3.

Does KJK/AtCSLD3 *play a role in morphogenesis of other cell types?*

The visible *kjk* phenotype is restricted to the root hairs. No pleiotropic defects in plant stature have been observed in *kjk* mutants as described previously for a number of other mutants with defective root hair growth. Plants homozygous for *tip1* and *rhd3* mutations are smaller than wild type, and *tip1* pollen growth is defective (Ryan et al. 1998; Schneider et al. 1998). This suggests that *KJK*, unlike many of the genes involved in root hair growth, is not required for the growth of other cells

throughout the plant. However, its expression in the shoot suggests that it is likely to be involved in the formation of complex polysaccharides in other cell types. The absence of shoot phenotypes in *kjk* mutants may be because of a compensation of its function in regular cell growth by other pathways or by redundancy of gene function.

Materials and methods

Plant materials and growth conditions

Seeds were grown on a 1:1 potting compost (John Innes No. 1):peat moss mix at 20°C with a 12-h day. For root hair observations, seeds were surface-sterilized for 5 min in 5% sodium hypochlorite and thoroughly rinsed in sterile distilled water. Seeds were placed on the surface of 0.5% phytagel (Sigma) solid medium containing 1% sucrose and MS salts at pH 5.8. Seeds were stratified at 4°C for 48 h in darkness and incubated at 24°C under continuous illumination. Plates were inclined at an angle of 60° to allow the roots to grow along the surface.

Mutant screening and genetic analysis

Arabidopsis thaliana (L.) Heyn. lines used in these experiments were derived from the Landsberg erecta (L*er*) and Columbia (Col) backgrounds. Seeds from a *Ds* transposon-mutagenized M_2 population (Bancroft et al. 1992) and an EMS M_2 population were plated on solid medium in Petri dishes, grown for 3–4 d, and screened for root hair mutant phenotypes. Putative mutants were transplanted and grown to maturity. M_3 seeds were plated on solid media in Petri dishes, seedlings were rescreened, and true breeding lines were maintained. Mutants were backcrossed to the wild type for four generations to eliminate other mutations from the background. For complementation tests and double mutant analysis, *kjk* was crossed to homozygous root hair mutants (*rhd1-1*, *rhd2-1*, *rhd3-1*, *rhd4-1*, *rhd6-1*, *cow1-1*, and *tip1-2*). The heterozygous F_1 families from each cross were scored and selfed and the F_2 populations were examined for putative double-mutant phenotypes. Putative double mutants were verified by in a backcross to both parents (testcross). *rhd1*, *rhd2*, *rhd3*, *rhd4*, and *rhd6* lines were kindly provided by John Schiefelbein, University of Michigan, Ann Arbor.

Analysis of root morphology and GFP imaging

Photographs of plants grown on phytagel medium were made using an Olympus SZH10 and a Wild M10 stereomicroscope. For cryo-scanning electron microscopy, plants were grown on phytagel medium and 3–5-d-old seedlings were placed on moist nitrocellulose paper mounted on a stub and immersed in liquid nitrogen slush. Roots were transferred to a cold stage. After removal of water by sublimation, roots were sputter coated with gold and observed using a JEOL Scanning Electron Microscope at –147°C. Roots were stained with 10 mg/mL propidium iodide and observed with a microscope Bio-Rad MRC 1024 or Leica TCS SP confocal laser scanning. A Leica TCS SP confocal laser scanning microscope was used to image GFP in transformed *Arabidopsis* and tobacco plants.

Genetic mapping

The *kjk-1* in the Landsberg erecta background was mapped in a cross to the wild-type Columbia strain. The F_2 population produced by selfing F_1 individuals was screened for Kjk^- phenotype. Simple sequence-length polymorphism (SSLP) (Bell and Ecker 1994) and cleaved amplified polymorphic sequences (CAPS) (Konieczny and Ausubel 1993) markers were used for mapping. DNA samples for the SSLP and CAPS mapping were prepared from single leaves of mutant F_2 plants (Doyle and Doyle 1990). All amplifications and restriction enzyme digestion of the resulting PCR products were performed as described previously (Konieczny and Ausubel 1993; Bell and Ecker 1994). The following primers and restriction enzymes were used: nga172, forward primer 5′-AGCTGCTTCCTTATAGCGTCC-3′ and reverse primer 5′-CATCCGAATGCCATTGTTC-3′; 17D8LE, forward primer 5′-CTCCTTTGTCATCTCCCGAATC-3′ and reverse primer 5′-CCAACAACATGCATGATAGTTCAG-3′ and polymorphism revealed by *Hin*cII; GAPC, forward primer 5′-CTGT TATCGTTAGGATTCGG-3′ reverse primer 5′-ACGGAAA GACATTCCAGTC-3′, and polymorphism revealed by *Eco*RV; CSL, forward primer 5′-GAGACTAGTGGGACTTACGGTT TC-3′ and reverse primer 5′-CTCACGCTTCACCCGTCTT CG-3′ and polymorphism revealed by *Taq*I.

Sequencing of mutant alleles

To sequence the *kjk* alleles, we amplified the *KJK/AtCSLD3* coding regions from wild-type and mutant plant tissues by PCR using a mix of Taq (GIBCO BRL) and Pwo polymerase (Boehringer Mannheim). The amplification condition were as follows: 3 min at 94°C, followed by 25 cycles of 30 sec at 94°C, 30 sec at 55°C, 1 min at 72°C, and a final extension at 72°C for 10 min. PCR products were used directly for sequencing. The alterations in sequence were verified by independent PCR amplifications. Nucleotide sequences were determined using the Ready Reaction ABI sequencing kit mix (Perkin Elmer).

Southern blot and Northern blot analysis

For Southern blot analysis, genomic DNA was isolated from 4-wk-old plants grown in vitro (Doyle and Doyle 1990). Southern blots were done using 5 μg of genomic DNA (Sambrook et al. 1989). For RNA analysis on wild-type and *kjk* mutants, total RNAs from leaves, roots, stems, and inflorescences were isolated using RNeasy Plant Minikit (Qiagen). For Northern blot analysis, RNA samples were separated in a formaldehyde containing agarose gel, blotted, and hybridized (Sambrook et al. 1989).

RACE and RT–PCR analysis

The 5′ and 3′ end of the *AtCSLD3* cDNA was obtained by RACE PCR (GIBCO BRL) with total RNA from the wild-type *A. thaliana* ecotype L*er* (Frohman et al. 1988). The primers CS4 5′-CACGGTCTGCTCATCAGATCCTGC-3′ and nested CS2 5′-CATCACCTTGACATCACAACCAG-3′ were used for 5′ RACE and primers CS9 5′-CGTTGGAATCTACCCGTTCA CATC-3′ and CS11 5′-GTGTGATTCCGCAGTGGAGTAA GT-3′ for 3′ RACE. The cDNA was also amplified with CS1 5′-GCTACAAAGTCCGGTGGATAGTGTT-3′ and CS12 5′-CTTGGCCAATCTCTGTCTCCATCTT-3′. PCR products were cloned in pGEM-T vector (Promega) and sequenced. For RT–PCR analysis, total RNAs were reverse transcribed with the oligo(dT) primer and were used as templates for PCR amplification. PCR reactions used CSL forward and reverse primers (see above) according to the following temperature profile (30 cycles): 94°C, 30 sec; 55°C, 30 sec; 72°C, 1 min. These primers produce a 740-bp fragment when cDNA is used as template and an 818-bp fragment when the genomic DNA is used.

Constructs and plant transformation

For the complementation of *kjk* mutation, a 7.2-kb *Avr*II fragment of the genomic DNA containing the *KJK/AtCSLD3* gene, its promoter, and its terminator was cloned into the pGreen0029 vector (Roger et al. 2000). DNA was isolated from BAC clone T17B22 (accession no. ATAC012328) by the alkaline method and its integrity confirmed by Southern blot analysis with probes from the *KJK/AtCSLD3* interval. This construct was introduced into *Agrobacterium tumefaciens* strain GV3101. The resulting strain was used to transform homozygous *kjk* mutant or L*er* plants by vacuum infiltration (Bechtold et al. 1993). Primary transformants were selected on MS medium containing 50 mg/L kanamycin and transferred to soil. Plants were grown to maturity and allowed to self.

Expression pattern of KJK

To identify in which cells *KJK/AtCSLD3* is expressed, the 5.0-kb *Avr*II–*Ase*I fragment containing the *KJK/AtCSLD3* gene and its promoter was fused in frame to an ER targeted *GFP2.5–nopaline synthase* terminator cassette in pGreen0229 (Roger et al. 2000). The construct was introduced into wild-type *Arabidopsis* as described above. The endoplasmic reticulum targeted GFP2.5 facilitates imaging cell-specific patterns, which can be problematic when using cytoplasmic GFPs. As a negative control, the promoterless GFP construct in pGreen 0229 was used.

Subcellular localization and Agrobacterium *infiltration*

For the subcellular localization of the KJK/AtCSLD3 protein, a 3.8-kb *Ssp*I–*Ase*I fragment of the *KJK/AtCSLD3* gene was fused in frame to a cytosolic *mGFP4* (Haseloff et al. 1995)—35S terminator cassette under the control of the 35S promoter in pGreen029 vector. We used the 35S CaMV promoter to control expression of the KJK/AtCSLD3::GFP4 fusion protein because it allows examination of the subcellular localization of the fusion in the large epidermal cells of tobacco. As controls, a cytosolic and an ER-targeted GFP4 under the control of the CaMV35S promoter were used. These constructs were introduced into *A. tumefaciens* strain GV3101. Infiltration of *Agrobacterium* into *N. benthamiana* was carried out as described (Voinnet and Baulcombe 1997).

Sequence analysis

The BLAST search program (Altschul et al. 1997) was used for sequence analysis and comparisons in the Genbank, EMBL, and swissProt databases at the National Center for Biotechnology Information (http://www.ncbi.nlm.nih.gov) and in the *Arabidopsis* Information Resource (TAIR) (http://www.arabidopsis.org/blast). For protein structure prediction, the following servers were used: TMHMM 1.0 (http://www.cbs.dtu.dk/services/TMHMM-1.0), TMDAS Transmembrane Prediction Server (http://www.biokemi.su.se/server/DAS/; Cserzo et al. 1997), TopPred (http://www.sbc.su.se/~erikw/toppred2; von Heijne 1992), PSort (http://psort.nibb.ac.jp), and DNA Strider 1.2 software. Multiple sequence alignments and the relationship tree were done with CLUSTAL W. All the sequences of the cellulose synthase homologs were retrieved from C. Somerville and T. Richmond's server (http://cellwall.stanford.edu/cellwall).

Accession number

The sequence data of the *A. thaliana* cellulose synthase-like *KJK/AtCSLD3* cDNA has been submitted to the DDBJ/EMBL/Genbank databases under accession no. AF232907.

Acknowledgments

We thank Silvia Costa for assistance with confocal microscopy, Todd Richmond and Chris Somerville for the cell wall carbohydrate analysis, Isabelle Malcuit and Patrick Laufs for help with GFP fusions, and Keith Roberts and Pierre Abad for critical reading of the manuscript. We acknowledge the input of three anonymous referees who helped us to highlight the importance of *KJK*. L.D. is grateful to Molly and Lew Tilney for help with preliminary experiments and valuable thoughts about how plant cells grow. We thank the Nottingham and Ohio Stock *Arabidopsis* stock centers for providing mutant seeds. BACs containing DNA from the Columbia accession of *Arabidopsis* were obtained from the *Arabidopsis* Biological Resource Center (ABRC) at Ohio State University. This work was supported by BBSRC, INRA, and the EU.

The publication costs of this article were defrayed in part by payment of page charges. This article must therefore be hereby marked "advertisement" in accordance with 18 USC section 1734 solely to indicate this fact.

References

Altschul, S.F., Madden, T.L., Schaffer, A.A., Zhang, J., Zhang, Z., Miller, W., and Lipman, D.J. 1997. Gapped BLAST and PSI-BLAST: A new generation of protein database search programs. *Nucleic Acids Res.* **25:** 3389–3402.

Arioli, T., Peng, L., Betzner, A.S., Burn, J., Wittke, W., Herth, W., Camilleri, C., Hofte, H., Plazinski, J., Birch, R., et al. 1998. Molecular analysis of cellulose biosynthesis in *Arabidopsis*. *Science* **279:** 717–720.

Bancroft, I., Bhatt, A.M., Sjodin, C., Scofield, S., Jones, J.D.G., and Dean, C. 1992. Development of an efficient two-element transposon tagging system in *Arabidopsis thaliana*. *Mol. Gen. Genet.* **233:** 449–461.

Bartel, B. and Fink, G.R. 1995. ILR1, an amidohydrolase that release active indole-3-acetic acid from conjugates. *Science* **268:** 1745–1748.

Bechtold, N., Elis, J., and Pelletier, G. 1993. In planta *Agrobacterium* mediated gene transfer by infiltration of adult *Arabidopsis thaliana*. *C.R. Acad. Sci. Paris* **316:** 1194–1199.

Bell, C.J. and Ecker, J.R. 1994. Assignment of 30 microsatellite loci to the linkage map of *Arabidopsis*. *Genomics* **19:** 137–144.

Bibikova, T.N., Jacob, T., Dahse, I., and Gilroy, S. 1998. Localized changes in apoplastic and cytoplasmic pH are associated with root hair development in *Arabidopsis thaliana*. *Development* **125:** 2925–2934.

Brown, R.M., Saxena, I.M., and Kudlicja, K. 1996. Cellulose biosynthesis in higher plants. *Trends Plant Sci.* **1:** 149–156.

Carpita, N. and Vergara, C. 1998. A recipe for cellulose. *Science* **279:** 672–673.

Cserzo, M., Wallin, E., Simon, I., von Heijne, G., and Elofsson, A. 1997. Prediction of transmembrane α-helices in procaryotic membrane proteins: The Dense Alignment Surface method. *Prot. Eng.* **10:** 673–676.

Cutler, S. and Somerville, C. 1997. Cellulose synthesis: Cloning in silico. *Curr. Genet.* **7:** R108–R111.

Delmer, D.P. 1999. Cellulose biosynthesis: Exciting times for a difficult field of study. *Annu. Rev. Plant Physiol. Mol. Biol.* **50:** 245–277.

Delmer, D.P., Reed, S.M., and Cooper, G. 1987. Identification of a receptor protein in cotton fibers for the herbicide 2,6-dichlorobenzonitrile. *Plant Physiol.* **84:** 415–420.

Dolan, L, Duckett, C., Grierson, C., Linstead, P., Schneider, K., Lawson, E., Dean, C., Poethig, S., and Roberts, K. 1994.

Clonal relationships and cell patterning in the root epidermis of *Arabidopsis*. *Development* **120:** 2465–2474.
Doyle, J.J. and Doyle, D.J. 1990. Isolation of plant DNA from fresh tissue. *Focus* **12:** 13–15.
Frohman, M.A., Dush, M.K., and Martin, G.R. 1988. Rapid production of full-length cDNAs from rare transcripts: Amplification using a single gene-specific oligonucleotide primer. *Proc. Natl. Acad. Sci.* **85:** 8998–9002.
Galway, M.E., Heckman, J.J.W., and Schiefelbein, J.W. 1997. Growth and ultrastructure of *Arabidopsis* root hairs: The *rhd3* mutation alters vacuole enlargement and tip growth. *Planta* **201:** 209–218.
Grierson, C.S., Roberts, K., Feldmann, K.A., and Dolan, L. 1997. The *COW1* locus of *Arabidopsis* acts after *RHD2* and in parallel with *RHD3* and *TIP1*, to determine the shape, rate of elongation, and number of root hairs produced from each site of hair formation. *Plant Physiol.* **115:** 981–990.
Haseloff, J., Siemering, K.R., Prasher, D.C., and Hodge, S. 1995. Removal of a cryptic intron and subcellular localization of green fluorescent protein are required to mark transgenic *Arabidopsis* plants brightly. *Proc. Natl. Acad. Sci.* **94:** 2122–2127.
Kimura, S., Laosinchain, W., Itoh, T., Cui, X., Linder, C.R., and Brown, R.M. 1999. Immunogold labeling of rosette terminal cellulose-synthesizing complexes in the vascular plant *Vigna angularis*. *Plant Cell* **11:** 2075–2085.
Konieczny, A. and Ausubel, F.M. 1993. A procedure for mapping *Arabidopsis* mutations using co-dominant ecotype-specific PCR-based markers. *Plant J.* **4:** 403–410.
Lee, M.M. and Schiefelbein, J. 1999. *WEREWOLF*, a MYB-related protein in *Arabidopsis*, is a position-dependent regulator of epidermal cell patterning. *Cell* **99:** 473–483.
Masucci, J.D. and Schiefelbein, J.W. 1994. The *rhd6* mutation of *Arabidopsis thaliana* alters root-hair initiation through an auxin- and ethylene-associated process. *Plant Physiol.* **106:** 1335–1346.
Mathur, J. and Chua, N.-H. 2000. Microtubule stabilization leads to growth reorientation in *Arabidopsis* trichomes. *Plant Cell* **12:** 465–478.
Oppenheimer, D.G., Pollock, M.A., Vacik, J., Szymanski, D.B., Ericson, B., Feldmann, K., and Marks, M.D. 1997. Essential role of a kinesin-like protein in *Arabidopsis* trichome morphogenesis. *Proc. Natl. Acad. Sci.* **94:** 6261–6266.
Pear, J.R., Kawagoe, Y., Schreckengost, W.E., Delmer, D.P., and Stalker, D.M. 1996. Higher plants contain homologs of the bacterial celA genes encoding the catalytic subunit of cellulose synthase. *Proc. Natl. Acad. Sci.* **93:** 12637–12642.
Roger, P., Hellens, E., Edwards, A., Leyland, N.R., Bean, S., and Mullineaux, P.M. 2000. pGreen: A versatile and flexible binary Ti vector for *Agrobacterium*-mediated plant transformation. *Plant Mol. Biol.* **42:** 819–832.
Ryan, E., Grierson, C.S., Cavell, A., Steer, M., and Dolan, L. 1998. *TIP1* is required for both tip growth and non-tip growth in *Arabidopsis*. *New Phytol.* **138:** 49–58.
Sambrook, J., Fritsch, E.F., and Maniatis, T. 1989. Molecular cloning: A laboratory manual. Cold Spring Harbor Laboratory Press, Cold Spring Harbor, NY.
Saxena, I.M., Brown, R.M., Fevre, M., Geremia, R.A., and Henrissat, B. 1995. Multidomain architecture of β-glycosyl transferases. *J. Bact.* **177:** 1419–1424.
Schiefelbein, J.W. and Somerville, C. 1990. Genetic control of root hair development in *Arabidopsis thaliana*. *Plant Cell* **2:** 235–243.
Schiefelbein, J.W., Shipley, A., and Rowse, P. 1992. Calcium influx at the tip of growing root-hair cells of *Arabidopsis thaliana*. *Plant J.* **187:** 455–459.
Schneider, K., Mathur, J., Boudonck, K., Wells, B., Dolan, L., and Roberts, K. 1998. The *ROOT HAIRLESS 1* gene encodes a nuclear protein required for root hair initiation in *Arabidopsis*. *Genes & Dev.* **12:** 2013–2021.
Taylor, N.G., Scheible, W.-R., Cutler, S., Somerville, C., and Turner, S.R. 1999. The *irregular xylem3* locus of *Arabidopsis* encodes a cellulose synthase required for secondary cell wall synthesis. *Plant Cell* **11:** 769–779.
Turner, S.R. and Somerville, C.R. 1997. Collapsed xylem phenotype of *Arabidopsis* identifies mutants deficient in cellulose deposition in the secondary cell wall. *Plant Cell* **9:** 689–701.
Voinnet, O. and Baulcombe, D.C. 1997. Systemic signaling in gene silencing. *Nature* **389:** 553.
von Heijne, G. 1992. Membrane protein structure prediction, hydrophobicity analysis and the positive-inside rule. *J. Mol. Biol.* **225:** 487–494.
Wang, H., Lockwood, S.K., Hoeltzel, M.F., and Schiefelbein, J.W. 1997. The *ROOT HAIR DEFECTIVE 3* gene encodes an evolutionarily conserved protein with GTP-binding motifs and is required for regulated cell enlargement in *Arabidopsis*. *Genes & Dev.* **11:** 799–811.
Wu, L., Joshi, C.P., and Chiang, V.L. 1998. *AraxCelA*, a new member of the cellulose synthase gene family from *Arabidopsis*. *Plant Physiol.* **117:** 1125.
Wymer, C.L., Bibikova, T.N., and Gilroy, S. 1997. Cytoplasmic free calcium distributions during the development of root hairs of *Arabidopsis thaliana*. *Plant J.* **12:** 427–439.

KOJAK encodes a cellulose synthase-like protein required for root hair cell morphogenesis in *Arabidopsis*

Bruno Favery, Eoin Ryan, Julia Foreman, et al.

Genes Dev. 2001, **15:**
Access the most recent version at doi:10.1101/gad.188801